

Limits on the hard x-ray emission from the periodic fast radio burst FRB 180916.J0158+65

Laha, Sibasish; Wadiasingh, Zorawar; Parsotan, Tyler; Lien, Amy; Younes, George; Zhang, Bing; Bradley Cenko, S.; Troja, Eleonora; Oates, Samantha; Nicholl, Matt; Meyer, Eileen; Becerra González, Josefa; Ghosh, Ritesh; Klingler, Noel

DOI:

[10.3847/1538-4357/ac5f3c](https://doi.org/10.3847/1538-4357/ac5f3c)

License:

Creative Commons: Attribution (CC BY)

Document Version

Publisher's PDF, also known as Version of record

Citation for published version (Harvard):

Laha, S, Wadiasingh, Z, Parsotan, T, Lien, A, Younes, G, Zhang, B, Bradley Cenko, S, Troja, E, Oates, S, Nicholl, M, Meyer, E, Becerra González, J, Ghosh, R & Klingler, N 2022, 'Limits on the hard x-ray emission from the periodic fast radio burst FRB 180916.J0158+65', *Astrophysical Journal*, vol. 929, no. 2, 173.
<https://doi.org/10.3847/1538-4357/ac5f3c>

[Link to publication on Research at Birmingham portal](#)

General rights

Unless a licence is specified above, all rights (including copyright and moral rights) in this document are retained by the authors and/or the copyright holders. The express permission of the copyright holder must be obtained for any use of this material other than for purposes permitted by law.

- Users may freely distribute the URL that is used to identify this publication.
- Users may download and/or print one copy of the publication from the University of Birmingham research portal for the purpose of private study or non-commercial research.
- User may use extracts from the document in line with the concept of 'fair dealing' under the Copyright, Designs and Patents Act 1988 (?)
- Users may not further distribute the material nor use it for the purposes of commercial gain.

Where a licence is displayed above, please note the terms and conditions of the licence govern your use of this document.

When citing, please reference the published version.






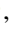






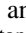

Take down policy

While the University of Birmingham exercises care and attention in making items available there are rare occasions when an item has been uploaded in error or has been deemed to be commercially or otherwise sensitive.

If you believe that this is the case for this document, please contact UBIRA@lists.bham.ac.uk providing details and we will remove access to the work immediately and investigate.



Limits on the Hard X-Ray Emission From the Periodic Fast Radio Burst FRB 180916.J0158+65

Sibasish Laha^{1,2,3} , Zorawar Wadiasingh^{2,3,4} , Tyler Parsotan^{1,2,3} , Amy Lien⁵ , George Younes² , Bing Zhang^{6,7} ,
S. Bradley Cenko^{2,8} , Eleonora Troja^{2,9} , Samantha Oates^{10,11} , Matt Nicholl^{10,11} , Eileen Meyer¹² ,
Josefa Becerra González^{13,14} , Ritesh Ghosh¹⁵ , and Noel Klingler^{1,2,3} 

¹ Center for Space Science and Technology, University of Maryland Baltimore County, 1000 Hilltop Circle, Baltimore, MD 21250, USA; sibasish.laha@nasa.gov, sib.laha@gmail.com

² Astrophysics Science Division, NASA Goddard Space Flight Center, Greenbelt, MD 20771, USA

³ Center for Research and Exploration in Space Science and Technology, NASA/GSFC, Greenbelt, MD 20771, USA

⁴ Department of Astronomy, University of Maryland, College Park, MD 20742, USA

⁵ University of Tampa, Department of Chemistry, Biochemistry, and Physics, 401 W. Kennedy Boulevard, Tampa, FL 33606, USA

⁶ Nevada Center for Astrophysics, University of Nevada, Las Vegas, NV 89154, USA

⁷ Department of Physics and Astronomy, University of Nevada Las Vegas, Las Vegas, NV 89154, USA

⁸ Joint Space-Science Institute, University of Maryland, College Park, MD 20742, USA

⁹ University of Rome Tor Vergata, Department of Physics, via della Ricerca Scientifica 1, I-00100, Rome, IT, Italy

¹⁰ School of Physics and Astronomy, University of Birmingham, Birmingham B15 2TT, UK

¹¹ Institute for Gravitational Wave Astronomy, University of Birmingham, Birmingham B15 2TT, UK

¹² Department of Physics, University of Maryland, Baltimore County, 1000 Hilltop Circle, Baltimore, MD 21250, USA

¹³ Instituto de Astrofísica de Canarias (IAC), E-38200 La Laguna, Tenerife, Spain

¹⁴ Universidad de La Laguna (ULL), Departamento de Astrofísica, E-38206 La Laguna, Tenerife, Spain

¹⁵ Inter-University Centre for Astronomy and Astrophysics (IUCAA), Pune, 411007, India

Received 2021 December 16; revised 2022 March 8; accepted 2022 March 11; published 2022 April 27

Abstract

FRB 180916.J0158+65 is one of the nearest, periodically repeating, and actively bursting fast radio bursts (FRBs) that has been localized to the outskirts of a spiral galaxy. In this work we study the FRB with the hard X-ray 14–195 keV data from the Burst Alert Telescope (BAT) on board The Neil Gehrels Swift Observatory. BAT uses coded mask technology giving a localization of $\lesssim 3'$ in the hard X-ray band, along with an accurate background estimation. BAT has been observing the source location in survey mode since 2020 February. The survey mode observations involve background subtracted spectra, integrated over a time span ranging 300–2000 s at the source location (from 2022 February–2022 January). We analyzed all the ~ 230 survey mode observations from BAT and checked for any signal in any of the observations. We did not detect any signal at $>5\sigma$ confidence level in any of the observations. We could estimate a 5σ upper limit on the 14–195 keV flux, which ranged between 4.5×10^{-10} – 7.6×10^{-9} erg cm⁻² s⁻¹. At the source distance this relates to a 5σ upper limit on a luminosity of 5.08×10^{44} – 8.5×10^{45} erg s⁻¹. With this estimate, we could rule out any persistent X-ray emission at the source location for these snapshots of BAT observations.

Unified Astronomy Thesaurus concepts: [Radio transient sources \(2008\)](#)

Supporting material: machine-readable table

1. Introduction

Fast radio bursts (FRBs) are bright, millisecond duration radio outbursts whose origin is still not clearly understood. To date, most FRBs possess dispersion measures larger than that of our own galaxy implying distances consistent with an extragalactic origin. In a few cases the host galaxies of these FRBs have been localized, e.g., FRB 121102 (Tendulkar et al. 2017), where the authors have found that it is located within a dwarf galaxy at a redshift of $z \sim 0.192$ and there is a faint persistent radio source of unknown origin at the FRB location (Chatterjee et al. 2017). Most FRBs have not been found to repeat. But deeper sky surveys such as CHIME/FRB are revealing an increasing number of repeater FRBs (CHIME/FRB Collaboration et al. 2019b; Fonseca et al. 2020; Amiri et al. 2021). It has been proposed that most FRBs that we

observe are actually repeaters because their all-sky rates largely exceed the all-sky rates of known cataclysmic events (see, e.g., Nicholl et al. 2017; Ravi 2019; Zhang 2020, and references therein).

FRB 180916 is one of the most well-known repeaters and also one of the most nearby FRBs detected to date. In 2019 December, the CHIME/FRB Collaboration reported the discovery of eight new repeating FRBs including FRB 180916, which was localized to a star-forming region of a nearby massive spiral galaxy at a redshift of $z = 0.0337 \pm 0.0002$ (Marcote et al. 2020). FRB 180916 exhibited ~ 38 radio bursts during 2019 September–2020 October, showing a clear periodicity of 16.35 ± 0.15 days, the first for any FRB. All the bursts arrived in a 5 day phase window and almost 50% of the bursts arrived in a 0.6 day phase window; these are the most active FRBs in the published CHIME/FRB sample (CHIME/FRB Collaboration et al. 2019a). The periodicity suggests a mechanism that periodically modulates the observed emission itself, or a periodic burst, or something else. Hence, this source is the focus of intense multiwavelength campaigns.

Table 1
List of Swift BAT Survey Mode Observations of FRB 180916, and the 5σ Upper Limit on the Fluxes in the Energy Band 14–195 keV

Obs ID	Pointing ID (number)	Start Time (MET)	Start Time (UTC) (year:day:hr:min:sec)	Exposure (s)	Flux Upper Limit ($\text{erg cm}^{-2} \text{s}^{-1}$)
00013201002	20200341843	602448230.0	2020 Feb 03 at 18:43:25	240.0	3.35e-09
00013201005	20200371529	602695795.0	2020 Feb 06 at 15:29:30	1088.0	2.32e-09
00013201006	20200381645	602786919.0	2020 Feb 07 at 16:48:14	684.0	2.81e-09
	20200381523	602781819.0	2020 Feb 07 at 15:23:14	1044.0	2.35e-09
00013201007	20200391516	602867799.0	2020 Feb 08 at 15:16:14	1044.0	2.39e-09
	20200391702	602874130.0	2020 Feb 08 at 17:01:45	233.0	4.99e-09
00013201008	20200561709	604343363.0	2020 Feb 25 at 17:08:58	300.0	2.51e-09
	20200561535	604337736.0	2020 Feb 25 at 15:35:11	179.0	1.62e-09
	20200561400	604332006.0	2020 Feb 25 at 13:59:41	177.0	5.90e-09
00013201009	20200651430	605111453.0	2020 Mar 05 at 14:30:28	600.0	4.00e-09
00013201011	20200671419	605283823.0	2020 Mar 07 at 14:23:18	300.0	5.38e-09
00013201014	20200701357	605541476.0	2020 Mar 10 at 13:57:31	1567.0	2.39e-09
00013201019	20200871153	607002839.0	2020 Mar 27 at 11:53:34	1744.0	2.31e-09
00013201021	20201141454	609346533.0	2020 Apr 23 at 14:55:08	150.0	8.09e-09
	20201141435	609345333.0	2020 Apr 23 at 14:35:08	900.0	3.60e-09
00013201023	20201161102	609505344.0	2020 Apr 25 at 11:01:59	1659.0	2.95e-09
00013201024	20201171055	609591323.0	2020 Apr 26 at 10:54:58	1660.0	2.96e-09
00013201025	20201181536	609694745.0	2020 Apr 27 at 15:38:40	1378.0	2.73e-09
00013201026	20201191526	609780416.0	2020 Apr 28 at 15:26:31	1687.0	2.50e-09
00013201027	20201201522	609866526.0	2020 Apr 29 at 15:21:41	1677.0	2.36e-09
00013201028	20201470743	612171836.0	2020 May 26 at 07:43:30	727.0	2.92e-09
	20201470915	612177309.0	2020 May 26 at 09:14:43	654.0	3.13e-09
00013201029	20201480730	612257414.0	2020 May 27 at 07:29:48	1069.0	2.44e-09
	20201480904	612263088.0	2020 May 27 at 09:04:22	855.0	2.91e-09
00013201030	20201490859	612349197.0	2020 May 28 at 08:59:31	666.0	3.11e-09
00013201031	20201500856	612435365.0	2020 May 29 at 08:55:39	478.0	3.61e-09
00013201032	20201510852	612521583.0	2020 May 30 at 08:52:37	240.0	5.105e-09
00013201034	20201630148	613532923.0	2020 Jun 11 at 01:48:17	560.0	3.52e-09
	20201630943	613561411.0	2020 Jun 11 at 09:43:05	1112.0	3.087e-09
00013201035	20201641554	613670061.0	2020 Jun 12 at 15:53:55	1302.0	2.42e-09
00013201036	20201652211	613779079.0	2020 Jun 13 at 22:10:53	1484.0	2.237e-09
00013201037	20201661402	613836136.0	2020 Jun 14 at 14:01:50	1727.0	2.16e-09
00013201038	20201671357	613922236.0	2020 Jun 15 at 13:56:50	1607.0	2.183e-09
00013201039	20201681350	614008228.0	2020 Jun 16 at 13:50:02	1595.0	2.11e-09
	20201682335	614043344.0	2020 Jun 16 at 23:35:18	439.0	3.88e-09
00013201040	20201692005	614117139.0	2020 Jun 17 at 20:05:13	1584.0	2.23e-09
00013201041	20201700231	614140312.0	2020 Jun 18 at 02:31:26	1691.0	2.25e-09
00013201043	20201800805	615024353.0	2020 Jun 28 at 08:05:27	600.0	3.32e-09
	20201800604	615017085.0	2020 Jun 28 at 06:04:19	1098.0	2.77e-09
00013201044	20201810613	615103998.0	2020 Jun 29 at 06:12:52	1005.0	2.85e-09
	20201810754	615110061.0	2020 Jun 29 at 07:53:55	762.0	3.03e-09
00013201045	20201820727	615194850.0	2020 Jun 30 at 07:27:04	333.0	4.60e-09
	20201820606	615189999.0	2020 Jun 30 at 06:06:13	1200.0	2.49e-09
00013201046	20201830410	615269416.0	2020 Jul 01 at 04:09:50	467.0	4.18e-09
	20201830603	615276238.0	2020 Jul 01 at 06:03:32	965.0	2.75e-09
00013201047	20201840559	615362370.0	2020 Jul 02 at 05:59:04	813.0	3.10e-09
00013201048	20201850553	615448424.0	2020 Jul 03 at 05:53:18	799.0	2.98e-09
00013201049	20201860550	615534625.0	2020 Jul 04 at 05:49:59	578.0	8.3e-10
00013201051	20201960600	616399216.0	2020 Jul 14 at 05:59:50	1007.0	3.00e-09
	20201960427	616393656.0	2020 Jul 14 at 04:27:10	687.0	3.42e-09
00013201052	20201970549	616484971.0	2020 Jul 15 at 05:49:05	1652.0	2.42e-09
00013201053	20201980551	616571487.0	2020 Jul 16 at 05:51:01	576.0	3.81e-09
	20201980419	616565963.0	2020 Jul 16 at 04:18:57	460.0	4.17e-09
00013201054	20201990539	616657157.0	2020 Jul 17 at 05:38:51	826.0	3.196e-09
00013201055	20202000531	616743121.0	2020 Jul 18 at 05:31:35	842.0	3.33e-09
	20202000356	616737379.0	2020 Jul 18 at 03:55:53	764.0	3.298e-09
00013201057	20202020347	616909656.0	2020 Jul 20 at 03:47:10	387.0	4.45e-09
	20202020523	616915431.0	2020 Jul 20 at 05:23:25	432.0	4.26e-09
00013201058	20202130447	617863661.0	2020 Jul 31 at 04:47:15	802.0	3.74e-09
	20202130311	617857887.0	2020 Jul 31 at 03:11:01	516.0	4.06e-09
00013201059	20202140437	617949461.0	2020 Aug 01 at 04:37:15	1282.0	3.12e-09
	20202140303	617943818.0	2020 Aug 01 at 03:03:12	505.0	4.40e-09
00013201060	20202150430	618035428.0	2020 Aug 02 at 04:30:02	1200.0	3.23e-09

Table 1
(Continued)

Obs ID	Pointing ID (number)	Start Time (MET)	Start Time (UTC) (year:day:hr:min:sec)	Exposure (s)	Flux Upper Limit ($\text{erg cm}^{-2} \text{s}^{-1}$)
00013201061	20202150255	618029745.0	2020 Aug 02 at 02:55:19	258.0	6.34e-09
	20202160425	618121550.0	2020 Aug 03 at 04:25:24	900.0	3.718e-09
00013201062	20202170416	618207380.0	2020 Aug 04 at 04:15:54	1200.0	3.0127e-09
00013201063	20202180409	618293397.0	2020 Aug 05 at 04:09:31	1200.0	2.9025e-09
00013201064	20202190402	618379338.0	2020 Aug 06 at 04:01:52	1200.0	2.627e-09
00013201065	20202290301	619239722.0	2020 Aug 16 at 03:01:36	1500.0	2.2564e-09
00013201066	20202300259	619325953.0	2020 Aug 17 at 02:58:47	300.0	1.94e-09
	20202300313	619326853.0	2020 Aug 17 at 03:13:47	351.0	4.289e-09
00013201067	20202310253	619412011.0	2020 Aug 18 at 02:53:05	1173.0	2.4877e-09
00013201075	20202450243	620621040.0	2020 Sep 01 at 02:43:34	1023.0	2.7753e-09
	20202450127	620616464.0	2020 Sep 01 at 01:27:18	799.0	3.1037e-09
00013201076	20202460233	620706802.0	2020 Sep 02 at 02:32:56	1481.0	2.439e-09
00013201077	20202470252	620794340.0	2020 Sep 03 at 02:51:54	223.0	5.8695e-09
	20202470227	620792840.0	2020 Sep 03 at 02:26:54	600.0	3.7665e-09
00013201079	20202490225	620965519.0	2020 Sep 05 at 02:24:53	524.0	3.803e-09
	20202490215	620964919.0	2020 Sep 05 at 02:14:53	600.0	3.612e-09
00013201080	20202500050	621046242.0	2020 Sep 06 at 00:50:16	862.0	1.07e-09
	20202500210	621051011.0	2020 Sep 06 at 02:09:45	300.0	1.14e-09
00013201081	20202510044	621132260.0	2020 Sep 07 at 00:43:54	823.0	3.15e-09
	20202510203	621137018.0	2020 Sep 07 at 02:03:12	865.0	2.9225e-09
00013201082	20202621247	622126051.0	2020 Sep 18 at 12:47:05	452.0	4.284e-09
00013201083	20202630129	622171746.0	2020 Sep 19 at 01:28:40	600.0	1.52e-09
00013201084	20202640120	622257621.0	2020 Sep 20 at 01:19:55	600.0	4.183e-09
00013201085	20202650112	622343567.0	2020 Sep 21 at 01:12:21	300.0	5.9935e-09
00013201086	20202660102	622429350.0	2020 Sep 22 at 01:02:04	1413.0	2.8653e-09
	20202660240	622435259.0	2020 Sep 22 at 02:40:33	244.0	1.99e-09
00013201087	20202670055	622515337.0	2020 Sep 23 at 00:55:11	900.0	3.3738e-09
00013201088	20202680048	622601317.0	2020 Sep 24 at 00:48:11	900.0	1.09e-09
	20202680104	622602517.0	2020 Sep 24 at 01:08:11	386.0	4.797e-09
00013201089	20202780123	623467428.0	2020 Oct 04 at 01:23:22	795.0	3.5332e-09
	20202780256	623472974.0	2020 Oct 04 at 02:55:48	649.0	3.748e-09
00013201090	20202790108	623552892.0	2020 Oct 05 at 01:07:46	291.0	5.9376e-09
00013201092	20202802325	623719559.0	2020 Oct 06 at 23:25:33	1684.0	2.4675e-09
00013201093	20202812317	623805468.0	2020 Oct 07 at 23:17:22	1755.0	2.4223e-09
00013201094	20202830045	623897158.0	2020 Oct 09 at 00:45:32	300.0	5.422e-09
	20202822329	623892555.0	2020 Oct 08 at 23:28:49	648.0	3.5875e-09
00013201095	20202850045	624069912.0	2020 Oct 11 at 00:44:46	531.0	3.962e-09
	20202842306	624063983.0	2020 Oct 10 at 23:05:57	1300.0	2.7107e-09
00013201096	20202960710	625043405.0	2020 Oct 22 at 07:09:39	1438.0	2.7067e-09
	20202960540	625038245.0	2020 Oct 22 at 05:43:39	959.0	3.256e-09
	20202960534	625037645.0	2020 Oct 22 at 05:33:39	300.0	5.359e-09
00013201097	20202970710	625129843.0	2020 Oct 23 at 07:10:17	1639.0	2.735e-09
00013201098	20202980839	625221570.0	2020 Oct 24 at 08:39:04	1593.0	2.5897e-09
00013201099	20202991142	625318925.0	2020 Oct 25 at 11:41:39	1738.0	2.517e-09
00013201100	20203001929	625433370.0	2020 Oct 26 at 19:29:04	1653.0	2.126e-09
00013201101	20203011759	625514363.0	2020 Oct 27 at 17:58:57	600.0	3.018e-09
00013201102	20203131851	626554315.0	2020 Nov 08 at 18:51:29	300.0	4.32e-09
	20203132200	626565653.0	2020 Nov 08 at 22:00:27	300.0	4.849e-09
	20203131716	626548616.0	2020 Nov 08 at 17:16:30	247.0	4.689e-09
	20203132031	626560256.0	2020 Nov 08 at 20:30:30	187.0	6.013e-09
00013201103	20203140731	626599904.0	2020 Nov 09 at 07:31:18	919.0	2.765e-09
00013201104	20203142018	626645888.0	2020 Nov 09 at 20:17:42	955.0	2.5645e-09
	20203142149	626651392.0	2020 Nov 09 at 21:49:26	1151.0	7.94e-10
00013201111	20203440406	629179624.0	2020 Dec 09 at 04:06:37	1319.0	2.524e-09
00013201112	20203450531	629271120.0	2020 Dec 10 at 05:31:33	1683.0	2.3245e-09
00013201113	20203481134	629552099.0	2020 Dec 13 at 11:34:32	1444.0	2.415e-09
00013201114	20203490816	629626618.0	2020 Dec 14 at 08:16:31	1565.0	2.519e-09
00013201115	20203501119	629723996.0	2020 Dec 15 at 11:19:29	900.0	3.0374e-09
00013201116	20203651817	631045081.0	2020 Dec 30 at 18:17:34	782.0	3.335e-09
	20203651956	631050977.0	2020 Dec 30 at 19:55:50	646.0	3.897e-09
00013201117	20203661959	631137568.0	2020 Dec 31 at 19:59:01	300.0	5.841e-09
	20203661808	631130943.0	2020 Dec 31 at 18:08:36	1260.0	2.591e-09
00013201118	20210011139	631193954.0	2021 Jan 01 at 11:38:47	649.0	3.2846e-09

Table 1
(Continued)

Obs ID	Pointing ID (number)	Start Time (MET)	Start Time (UTC) (year:day:hr:min:sec)	Exposure (s)	Flux Upper Limit (erg cm ⁻² s ⁻¹)
00013201119	20210010827	631182432.0	2021 Jan 01 at 08:26:45	1311.0	2.5016e-09
	20210100240	631939239.0	2021 Jan 10 at 02:40:12	1764.0	2.389e-09
00013201120	20210110233	632025217.0	2021 Jan 11 at 02:33:10	1766.0	2.3602e-09
00013201121	20210122136	632180188.0	2021 Jan 12 at 21:36:01	1595.0	2.2733e-09
00013201122	20210131951	632260302.0	2021 Jan 13 at 19:51:15	1701.0	2.40e-09
	20210132127	632266051.0	2021 Jan 13 at 21:27:04	1712.0	2.20e-09
00013201123	20210141634	632334864.0	2021 Jan 14 at 16:33:57	1719.0	2.4425e-09
00013201124	20210151938	632432312.0	2021 Jan 15 at 19:38:05	1711.0	2.3778e-09
00013201125	20210160213	632455971.0	2021 Jan 16 at 02:12:24	300.0	5.7285e-09
	20210160157	632455071.0	2021 Jan 16 at 01:57:24	300.0	5.201e-09
00013201132	20210331559	633974372.0	2021 Feb 02 at 15:59:05	287.0	2.7897e-09
00013201134	20210621452	636475946.0	2021 Mar 03 at 14:51:59	637.0	3.995e-09
00013201136	20210641324	636643500.0	2021 Mar 05 at 13:24:33	483.0	1.94e-09
00013201139	20210771309	637765766.0	2021 Mar 18 at 13:08:59	300.0	5.444e-09
00013201142	20210801305	638024954.0	2021 Mar 21 at 13:08:47	409.0	4.538e-09
00013201143	20210811240	638109627.0	2021 Mar 22 at 12:40:00	1716.0	2.37e-09
00013201145	20211091202	640526551.0	2021 Apr 19 at 12:02:26	212.0	6.509e-09
00013201146	20211101131	640611085.0	2021 Apr 20 at 11:31:20	1658.0	2.618e-09
00013201147	20211111124	640697088.0	2021 Apr 21 at 11:24:43	1635.0	2.6705e-09
00013201148	20211121117	640783039.0	2021 Apr 22 at 11:17:14	1484.0	2.753e-09
	20211121610	640800645.0	2021 Apr 22 at 16:10:40	678.0	3.474e-09
00013201149	20211130001	640828877.0	2021 Apr 23 at 00:01:12	300.0	4.806e-09
	20211131110	640869039.0	2021 Apr 23 at 11:10:34	1644.0	2.5765e-09
	20211130009	640829477.0	2021 Apr 23 at 00:11:12	166.0	6.636e-09
00013201150	20211141107	640955238.0	2021 Apr 24 at 11:07:13	1605.0	2.519e-09
00013201151	20211151100	641041209.0	2021 Apr 25 at 11:00:04	1614.0	2.559e-09
	20211150436	641018178.0	2021 Apr 25 at 04:36:13	1005.0	2.917e-09
00013201153	20211290922	642244925.0	2021 May 09 at 09:22:00	600.0	3.751e-09
	20211291055	642250528.0	2021 May 09 at 10:55:23	600.0	3.76e-09
00013201154	20211300908	642330541.0	2021 May 10 at 09:08:56	970.0	2.9134e-09
00013201155	20211311051	642423373.0	2021 May 11 at 10:56:08	350.0	4.7754e-09
00013201159	20211441041	643545682.0	2021 May 24 at 10:41:17	278.0	5.653e-09
	20211440911	643540283.0	2021 May 24 at 09:11:18	460.0	4.28e-09
00013201160	20211450555	643614931.0	2021 May 25 at 05:55:26	582.0	3.3717e-09
00013201161	20211580807	644746078.0	2021 Jun 07 at 08:07:53	1385.0	2.673e-09
00013201162	20211590800	644832053.0	2021 Jun 08 at 08:00:48	1200.0	2.7623e-09
00013201163	20211600753	644918000.0	2021 Jun 09 at 07:53:15	1200.0	2.908e-09
00013201164	20211610746	645004014.0	2021 Jun 10 at 07:46:49	1200.0	2.9817e-09
00013201165	20211620740	645090007.0	2021 Jun 11 at 07:40:02	1200.0	2.8246e-09
00013201166	20211630732	645175978.0	2021 Jun 12 at 07:32:53	1200.0	2.779e-09
00013201167	20211640724	645261882.0	2021 Jun 13 at 07:24:37	1461.0	2.6162e-09
00013201169	20211730447	646030030.0	2021 Jun 22 at 04:47:05	1200.0	2.7585e-09
	20211730510	646031530.0	2021 Jun 22 at 05:12:05	173.0	6.483e-09
00013201170	20211740745	646127135.0	2021 Jun 23 at 07:45:30	1708.0	2.1495e-09
00013201171	20211750620	646208442.0	2021 Jun 24 at 06:20:37	1041.0	2.642e-09
00013201172	20211761548	646328943.0	2021 Jun 25 at 15:48:58	360.0	4.869e-09
	20211770908	646391293.0	2021 Jun 26 at 09:08:08	710.0	3.3605e-09
	20211761856	646340223.0	2021 Jun 25 at 18:56:58	840.0	3.0734e-09
	20211772334	646443271.0	2021 Jun 26 at 23:34:26	512.0	4.242e-09
	20211760602	646293757.0	2021 Jun 25 at 06:02:32	1707.0	2.2164e-09
00013201173	20211780424	646460698.0	2021 Jun 27 at 04:24:53	545.0	3.6787e-09
	20211780719	646471186.0	2021 Jun 27 at 07:19:41	737.0	3.207e-09
	20211790904	646563890.0	2021 Jun 28 at 09:04:45	853.0	2.981e-09
00013201174	20211790535	646551329.0	2021 Jun 28 at 05:35:24	1114.0	2.835e-09
	20211790711	646557091.0	2021 Jun 28 at 07:11:26	392.0	4.593e-09
	20211890605	647417112.0	2021 Jul 08 at 06:05:07	1431.0	4.57e-10
00013201175	20211900554	647502881.0	2021 Jul 09 at 05:54:36	1702.0	2.365e-09
00013201176	20211910729	647594963.0	2021 Jul 10 at 07:29:18	460.0	4.218e-09
	20211910555	647589325.0	2021 Jul 10 at 05:55:20	1238.0	2.5826e-09
00013201178	20211920542	647674932.0	2021 Jul 11 at 05:42:07	951.0	3.031e-09
00013201180	20211940217	647835482.0	2021 Jul 13 at 02:17:57	781.0	3.2184e-09
	20211940531	647847077.0	2021 Jul 13 at 05:31:12	706.0	3.4086e-09
00013201181	20211950659	647938771.0	2021 Jul 14 at 06:59:26	812.0	3.408e-09

Table 1
(Continued)

Obs ID	Pointing ID (number)	Start Time (MET)	Start Time (UTC) (year:day:hr:min:sec)	Exposure (s)	Flux Upper Limit (erg cm ⁻² s ⁻¹)
00013201182	20211950525	647933106.0	2021 Jul 14 at 05:25:01	597.0	1.54e-09
	20212060447	648881252.0	2021 Jul 25 at 04:47:27	391.0	5.223e-09
	20212060621	648886885.0	2021 Jul 25 at 06:21:20	459.0	5.304e-09
00013201183	20212070614	648972868.0	2021 Jul 26 at 06:14:23	600.0	4.791e-09
	20212070439	648967168.0	2021 Jul 26 at 04:39:23	875.0	3.613e-09
00013201184	20212080431	649053124.0	2021 Jul 27 at 04:31:59	1139.0	3.385e-09
	20212080607	649058880.0	2021 Jul 27 at 06:07:55	244.0	7.674e-09
00013201185	20212090419	649138798.0	2021 Jul 28 at 04:19:53	1500.0	2.9306e-09
00013201186	20212100413	649224800.0	2021 Jul 29 at 04:13:15	1723.0	2.727e-09
00013201187	20212110410	649311053.0	2021 Jul 30 at 04:10:48	1270.0	3.1487e-09
00013201188	20212121021	649419943.0	2021 Jul 31 at 10:25:38	600.0	4.162e-09
00013201189	20212560558	653205519.0	2021 Sep 13 at 05:58:34	264.0	6.923e-09
00013201191	20212600035	653531755.0	2021 Sep 17 at 00:35:50	300.0	6.383e-09
	20212600050	653532655.0	2021Sep17 at 00:50:50	300.0	5.919e-09
00013201199	20212760010	654912618.0	2021 Oct 03 at 00:10:13	1665.0	2.19e-09
00013201200	20212770003	654998591.0	2021 Oct 04 at 00:03:06	300.0	4.91e-09
00013201201	20212771745	655062358.0	2021 Oct 04 at 17:45:53	1325.0	2.526e-09
00013201202	20212780131	655090278.0	2021 Oct 05 at 01:31:13	1665.0	2.1616e-09
00013201203	20212912230	656289186.0	2021 Oct 18 at 22:33:01	477.0	4.265e-09
	20212912218	656288286.0	2021Oct18 at 22:18:01	600.0	1.54e-09
00013201204	20213072113	657666951.0	2021 Nov 03 at 21:15:46	192.0	6.118e-09
00013201205	20213082235	657758161.0	2021 Nov 04 at 22:35:56	300.0	5.638e-09
00013201207	20213102215	657929752.0	2021 Nov 06 at 22:15:47	1200.0	2.9644e-09
00013201210	20213232044	659047485.0	2021 Nov 19 at 20:44:40	900.0	3.343e-09
00013201211	20213242041	659133687.0	2021 Nov 20 at 20:41:22	1200.0	2.875e-09
00013201214	20213362039	660170354.0	2021 Dec 02 at 20:39:09	1369.0	2.3474e-09
00013201215	20213372031	660256279.0	2021 Dec 03 at 20:31:14	1304.0	2.289e-09
00013201216	20213382036	660342979.0	2021 Dec 04 at 20:36:14	1364.0	2.1998e-09
00013201217	20213392016	660428224.0	2021 Dec 05 at 20:16:59	1679.0	2.0684e-09
00013201218	20213402009	660514188.0	2021 Dec 06 at 20:09:43	1694.0	2.1318e-09
00013201219	20213412003	660600200.0	2021 Dec 07 at 20:03:15	1663.0	2.141e-09
00013201220	20213421955	660686158.0	2021 Dec 08 at 19:55:53	1685.0	2.207e-09
00013201221	20213591835	662150105.0	2021 Dec 25 at 18:35:00	1018.0	2.785e-09
00013201224	20220041732	663010338.0	2022 Jan 04 at 17:32:13	1005.0	3.1497e-09
	20220041855	663015305.0	2022 Jan 04 at 18:55:00	898.0	3.3017e-09
00013201225	20220051722	663096183.0	2022 Jan 05 at 17:22:58	960.0	3.1152e-09
	20220051847	663101271.0	2022 Jan 05 at 18:47:46	852.0	5.12e-09
00013201226	20220061700	663181256.0	2022 Jan 06 at 17:00:51	1147.0	3.1096e-09
	20220061840	663187256.0	2022 Jan 06 at 18:40:51	547.0	4.237e-09
00013201227	20220071831	663273119.0	2022 Jan 07 at 18:31:54	1624.0	7.94e-10
00013201228	20220081823	663359039.0	2022 Jan 08 at 18:23:54	1684.0	2.4566e-09
00013201229	20220091815	663444962.0	2022 Jan 09 at 18:15:57	1681.0	2.415e-09
00013201230	20220101807	663530826.0	2022 Jan 10 at 18:07:01	1677.0	2.385e-09

Note. These data sets are all publicly available in the HEASARC archive as of 2022 January 15. The start times of the observations are given in two units: mission elapsed time (MET) and Coordinated Universal Time (UTC).

(This table is available in its entirety in machine-readable form.)

High-energy emission from magnetars has long been thought to be one of the important mechanisms by which FRBs may also be generated (see Margalit et al. 2020, and references therein). The recent discovery of the connection between FRB 200428 and SGR 1935 (CHIME/FRB Collaboration et al. 2020; Margalit et al. 2020; Mereghetti et al. 2020; Younes et al. 2020; Li et al. 2021; Kirsten et al. 2021; Younes et al. 2021) confirmed this fact that at least some FRBs are produced by magnetar short bursts. The typical radio to X-ray fluence measured was $\eta \equiv E_R/E_X \sim 10^{-5}$, implying that the radio emission is weak and contributes little to the overall burst energy budget. Moreover the radio fluence of FRB 200428 was somewhat lower compared to its extragalactic counterparts (the

STARE2 burst energetics however have a strictly lower limit since some of the burst appears to be out of band). Variable high-energy emission at different timescales (milliseconds to years) is one of the key features of magnetars, and may have a relation to FRB emission (Palmer et al. 2005; Younes et al. 2015; Coti Zelati et al. 2018; Younes et al. 2020).

Here we discuss the three most common types of emission phenomenology from magnetars. First, the flares associated with the short bursts, which can be bright ($L_X \leq 10^{42}$ erg s⁻¹) and last a few hundreds of milliseconds; these short bursts may happen in isolation, or during a burst storm when hundreds of them are detected, continuing for days. Second, magnetars can exhibit giant flares, which consist of a very bright pulse

($L_X \leq 10^{47}$ erg s⁻¹) at submillisecond level, followed by a softer pulsating tail lasting for several minutes. These events have been detected in three Galactic magnetars (e.g., SGR 1806; Mazets et al. 1979; Hurley et al. 1999; Palmer et al. 2005). Third, on longer timescales, magnetars recurrently enter outburst phases when their persistent flux level increases by orders of magnitude accompanied by random spectral and temporal variability. These phases often persist for a few months to years, after which they recover to their pre-outburst levels. In this work we focus on detecting the second and third kinds of emission from a putative extragalactic magnetar powering FRB 180916. Swift Burst Alert Telescope (BAT) survey observations, which cover the energy range 14–195 keV and have a time integration of a few hundreds of seconds, can constrain to models of young magnetars undergoing giant flares.

Several works studying the X-rays to γ -rays have put upper limits on the possible nondetection from the sky location of FRB 180916. Verrecchia et al. (2021) using AGILE in the energy range 0.4 MeV–30 GeV could put an upper limit on the total hard X-ray energy of $\sim 10^{46}$ erg s⁻¹ comparable to that of SGR 1806-20. Although the extragalactic FRBs emit radio pulses of energies that are significantly larger than that detected from SGR 1935, there are no simultaneous or contemporaneous detections of keV, MeV, or GeV photons to date. Contemporaneous X-ray and radio observations of FRB 180916 were carried out by Scholz et al. (2020), with CHIME and the Chandra X-ray Observatory. They detected no X-ray events in excess of the background, and the nondetections imply a 5σ fluence limit of $< 5 \times 10^{-10}$ erg cm⁻² in the 0.5–10 keV energy range during the prompt emission and $< 1.3 \times 10^{-9}$ erg cm⁻² at any time during the observations. Given the cosmological distance of this FRB, these relate to the total isotropic energies $< 1.6 \times 10^{45}$ erg and $< 4 \times 10^{45}$ erg, respectively. In the 10–100 keV Fermi Gamma Ray Burst Monitor (GBM) observations, the search for prompt emission (Scholz et al. 2020) led to a fluence upper limit of 9×10^{-9} erg cm⁻². Tavani et al. (2020) searched for contemporaneous γ -ray emission from FRB 180916 using AGILE and X-ray emission using the X-Ray Telescope (XRT) on board The Neil Gehrels Swift Observatory (Swift from now on), during the bursting phases of the source in 2020 February and 2020 March. They did not detect any hard X-ray or γ -ray photons, and could provide a persistent flux upper limit of 5×10^{-14} erg cm⁻² s⁻¹, which translates to an isotropic luminosity of $L_X \sim 1.5 \times 10^{41}$ erg s⁻¹. Guidorzi et al. (2020) using the Insight-Hard X-ray Modulation Telescope (Insight-HXMT) could provide a prompt emission upper limit in hard X-rays (1–100 keV) of $< 10^{46}$ erg over a timescale of $\Delta t < 0.1$ s. They could rule out giant flares similar to the ones that were observed in Galactic magnetars.

FRB sources like magnetars may emit the majority of their flux at photon energies > 10 keV (Woods & Thompson 2006; Turolla et al. 2015; Scholz et al. 2017; Margalit et al. 2020). To study the possible hard X-ray emission in the 14–195 keV energy band, we analyze all the available survey mode observations from BAT on board Swift. BAT’s well-suited energy range (14–195 keV) coupled with hundreds of pointing on the source over a period extending from 2020 February–2022 January, serves as a unique opportunity for us to capture any hard X-ray emission from FRB 180916 and/or put upper

limits on the short-term (hundreds of seconds) or long-term (\sim year) persistent X-ray emission from the source.

The paper is arranged as follows: Section 2 discusses the observations and data analysis. Section 3 discusses the results, followed by conclusions in Section 4.

2. Observation and Data Analysis

FRB 180916 has been observed by Swift BAT (Gehrels et al. 2004; Barthelmy et al. 2005) ~ 220 times from 2020 February–2022 January in survey mode. We checked in the CHIME/FRB catalog (Amiri et al. 2021) for the time stamps of the ~ 90 radio bursts detected to date from FRB 180916. Unfortunately, none of the CHIME-reported burst times were coincident with our BAT survey observations. We also note that there are no time-tagged event data available in the BAT archive where FRB 180916 is in the field of view of BAT. For out-of-field-of-view sources, the response matrix of BAT is highly uncertain and hence any measurement of flux is associated with large errors, hence we did not use them in this work. Below we describe the methods used to obtain the survey data sets, and to reprocess and analyze them. We have extensively used *batsurvey* from HEASOFT.

The BAT survey mode data are also known as detector plane histograms or DPHs. As opposed to event data, BAT survey data are accumulated in histograms on board the spacecraft, with typical integration times of 300 s or more. An 80-channel binned spectrum is recorded for each of the active detectors and saved in the DPH files. In this work we use all the available BAT data sets and we explain below the steps we have taken to reprocess and analyze them (see Table 1 for a full list of observations).

The BAT survey data sets were downloaded from HEASARC, and every survey observation has one or more pointings and hence different integration times. The task *batsurvey* performs basic analysis of BAT survey data and reduces a set of “raw” observed DPHs. Most importantly, it performs data screening that the BAT team has found vital for obtaining good quality results. It produces sky images and source fluxes for each independent “snapshot,” corresponding to a single pointed visit by BAT. We chose a set of eight independent energy bins, and *batsurvey* recorded the images and fluxes in each of those bands separately. *Batsurvey* operates on a single BAT observation. For multiple observations, we used *batsurvey* once for each observation. We provided the source R.A. and decl. in the catalog, which were used as an input to *batsurvey*.

The output from *batsurvey* gives us exposure-specific results. For example, one of the important files produced for each pointing is the flux catalog. This catalog contains sources listed in the input catalog (which in this case includes FRB 180916) as well as sources detected by a blind search. From this file, we create the lightcurve for the source FRB 180916 using the command “*batsurvey-catmux*.” We then extract the Tstart, and ΔT from the lightcurve and obtain the time-integrated spectrum with eight energy channels.

In the first round, to generate the source spectrum we choose “CENT-RATE” as the column for rate array, and use the background variance (BKG-VAR) for the error on the rate. We note that the source spectrum is already background subtracted due to the coded mask technique; hence sometimes when the background variance is larger than the “net source” counts, then the count rate may become negative. Once the spectrum is obtained we obtain the response matrix using the task

“batdrngen”. We used the model `cflux*powerlaw` in XSPEC notation to estimate the flux in the 14–195 keV energy band. We froze the power-law normalization to a value of $1e-03$ and kept the power-law slope (Γ) free, in order to calculate the flux using the model above. We did not detect any excess emission above the background (at a $>5\sigma$ confidence) in any of the pointings of this source.

In the second round, we reextracted the spectrum for every pointing, now using the $5 \times$ BKG-VAR as the rate array. Here we use a simple `powerlaw` model with $\Gamma=1$ fixed, to estimate the flux in the 14–195 keV energy range. Note that this is the 5σ upper limit on the background variance and hence the 5σ upper limit on the flux. In Table 1 we quote the 5σ upper limit on the 14–195 keV flux obtained for all the available BAT pointings. To carry out all the above steps in a coherent way, we developed a user-friendly pipeline in python, which will be published in the near future.

3. Results and Discussion

We have carried out a hard X-ray counterpart search of FRB 180916 using survey mode observations of BAT on board Swift. We have analyzed all available observations as of 2022 January 15 using standard analysis methods. We do not detect any source signal in excess of the background with $>5\sigma$ significance. The 5σ upper limit on the background flux range from 4.5×10^{-10} – 7.6×10^{-9} erg cm $^{-2}$ s $^{-1}$ for different pointings of BAT survey observations. At the source distance this relates to a 5σ upper limit on a luminosity of 5.08×10^{44} – 8.5×10^{45} erg s $^{-1}$. Below we discuss our results in context to previous estimates of X-ray limits on this source and also discuss the possible progenitor scenarios. We note that the CHIME-measured fluences for this FRB vary considerably, and one representative value is ~ 27 Jy ms (for burst ID: 181222 in the CHIME catalog). Unfortunately, we did not have any simultaneous CHIME and BAT (in field-of-view) observations.

Observations with the AGILE telescope (Tavani et al. 2021), working in the energy range 400 keV–100 MeV, could constrain the bursting X-ray energy of FRB 180916 to $\sim 10^{46}$ erg, which is smaller than that observed from giant flares from Galactic magnetars. Similar upper limits of $\sim 10^{46}$ erg on the bursting energy of FRB 180916 were obtained using Insight-HMXT in the energy range 1–100 keV (Guidorzi et al. 2020). On the soft X-ray range 0.3–10 keV strong limits on persistent luminosity ($< 2 \times 10^{40}$ erg s $^{-1}$) and prompt emission fluence ($< 5 \times 10^{-10}$ erg cm $^{-2}$) could be obtained during the bursting phases of FRB 180916 using observations from Chandra (Scholz et al. 2020). Similarly, Tavani et al. (2020) could put a cumulative upper limit on the X-ray flux using Swift XRT observations $F < 5 \times 10^{-14}$ erg cm $^{-2}$ s $^{-1}$, obtained during the 5 day active period of the source. These clearly rule out magnetar giant flares and/or SGR 1935 type events.

The Swift BAT flux upper limits in 14–195 keV obtained in this work, which are of a few $\times 10^{-9}$ erg cm $^{-2}$ s $^{-1}$, correspond to a luminosity limit of about $\sim 10^{45}$ erg s $^{-1}$ at the source location (that is at 149 Mpc). We discuss the following three progenitor scenarios:

1. *Magnetar Giant Flares (MGFs)*. Typical magnetar giant flares with a luminosity $\sim 10^{47}$ erg s $^{-1}$, lasting for ~ 0.1 s (Burns et al. 2021), would lead to an average luminosity of $\sim 10^{43}$ erg s $^{-1}$, when averaged over 1000 s of a typical

BAT survey observation. This would correspond to a flux of $\sim 4 \times 10^{-12}$ erg cm $^{-2}$ s $^{-1}$. This flux level is well below the flux level that BAT is sensitive to, and hence we cannot rule out an MGF event.

2. *Pulsating Tails of MGFs*. The pulsating tails have a typical luminosity of 10^{42} erg s $^{-1}$, and their peak energy lies in the BAT energy range, and they extend for several seconds (Younes et al. 2020; Burns et al. 2021). The corresponding flux emitted by such pulsating tails would be $\sim 10^{-13}$ erg cm $^{-2}$ s $^{-1}$, which is well below the flux level that BAT is sensitive to.
3. *An SGR 1935 Type Event*. For such an event happening at the location of FRB 180916 the expected 20–200 keV flux is about a few $\times 10^{-14}$ erg cm $^{-2}$ s $^{-1}$ (Mereghetti et al. 2020; Li et al. 2021). This flux level is also well below the flux level that BAT is sensitive to, and hence we cannot rule out an event like SGR 1935.

Our limits exclude any persistent emission or transient activity with the source position down to $\sim 10^{45}$ erg s $^{-1}$. The possible progenitor of FRB 180916 might be older than canonical magnetars, based on the offset reported in Tendulkar et al. (2021). The authors suggest that the spatial offset and hence the timescale (of travel from its presumed birth site) points more toward high-mass X-ray binaries and gamma-ray binaries, rather than magnetars. Given the unpredictable nature of FRBs and magnetars, such multiband long-term monitoring snapshots are extremely useful. Future opportunities with prompt downlink and analysis of Swift BAT time-tagged event data of FRBs (GUANO; Tohuvavohu et al. 2020; DeLaunay & Tohuvavohu 2021), contemporaneous with radio bursts, will open up new avenues of hard X-ray follow-up of these hitherto unknown phenomena.

4. Conclusions

We searched for high-energy transients in Swift BAT survey mode data associated with FRB 180916 from 2020 February to 2022 January. We did not detect any significant emission in the 14–195 keV energy band in any of our observational snapshots when FRB 180916 was in the field of view of BAT. The upper limits on the flux estimated in these observations exclude any persistent emission or transient activity with the source position down to $\sim 10^{45}$ erg s $^{-1}$, for all the snapshots. Our results confirm and corroborate previous limits of high-energy transients by Fermi GBM, AGILE, HXMT-Insight, and XMM-Newton.

The material is based upon work supported by NASA under award No. 80GSFC21M0002. E.T. acknowledges support from NASA grant 80NSSC18K0429. M.N. is supported by the European Research Council (ERC) under the European Unions Horizon 2020 research and innovation program (grant agreement No. 948381) and by a Fellowship from the Alan Turing Institute.

ORCID iDs






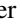
Sibasish Laha  <https://orcid.org/0000-0003-2714-0487>

Zorawar Wadiasingh  <https://orcid.org/0000-0002-9249-0515>

Tyler Parsotan  <https://orcid.org/0000-0002-4299-2517>

Amy Lien  <https://orcid.org/0000-0002-7851-9756>

George Younes  <https://orcid.org/0000-0002-7991-028X>

Bing Zhang  <https://orcid.org/0000-0002-9725-2524>
 S. Bradley Cenko  <https://orcid.org/0000-0003-1673-970X>
 Eleonora Troja  <https://orcid.org/0000-0002-1869-7817>
 Samantha Oates  <https://orcid.org/0000-0001-9309-7873>
 Matt Nicholl  <https://orcid.org/0000-0002-2555-3192>
 Eileen Meyer  <https://orcid.org/0000-0002-7676-9962>
 Josefa Becerra González  <https://orcid.org/0000-0002-6729-9022>
 Ritesh Ghosh  <https://orcid.org/0000-0003-4790-2653>
 Noel Klingler  <https://orcid.org/0000-0002-7465-0941>

References

- Amiri, M., Andersen, B. C., Bandura, K., et al. 2021, *ApJS*, 257, 59
 Barthelmy, S. D., Barbier, L. M., Cummings, J. R., et al. 2005, *SSRv*, 120, 143
 Burns, E., Svinkin, D., Hurley, K., et al. 2021, *ApJ*, 907, L28
 Chatterjee, S., Law, C. J., Wharton, R. S., et al. 2017, *Nat*, 541, 58
 CHIME/FRB Collaboration, Andersen, B. C., Bandura, K., et al. 2019a, *ApJL*, 885, L24
 CHIME/FRB Collaboration, Andersen, B. C., Bandura, K., et al. 2019b, *ApJ*, 885, L24
 CHIME/FRB Collaboration, Andersen, B. C., Bandura, K. M., et al. 2020, *Nat*, 587, 54
 Coti Zelati, F., Rea, N., Pons, J. A., Campana, S., & Esposito, P. 2018, *MNRAS*, 474, 961
 DeLaunay, J., & Tohuvavohu, A. 2021, arXiv:2111.01769
 Fonseca, E., Andersen, B. C., Bhardwaj, M., et al. 2020, *ApJ*, 891, L6
 Gehrels, N., Chincarini, G., Giommi, P., et al. 2004, *ApJ*, 611, 1005
 Guidorzi, C., Orlandini, M., Frontera, F., et al. 2020, *A&A*, 642, A160
 Hurley, K., Cline, T., Mazets, E., et al. 1999, *Nat*, 397, 41
 Kirsten, F., Snelders, M. P., Jenkins, M., et al. 2021, *NatAs*, 5, 414
 Li, C. K., Lin, L., Xiong, S. L., et al. 2021, *NatAs*, 5, 378
 Marcote, B., Nimmo, K., Hessels, J. W. T., et al. 2020, *Natur*, 577, 190
 Margalit, B., Beniamini, P., Sridhar, N., & Metzger, B. D. 2020, *ApJ*, 899, L27
 Mazets, E. P., Golentskii, S. V., Ilinskii, V. N., Aptekar, R. L., & Guryan, I. A. 1979, *Nat*, 282, 587
 Mereghetti, S., Savchenko, V., Ferrigno, C., et al. 2020, *ApJ*, 898, L29
 Nicholl, M., Williams, P. K. G., Berger, E., et al. 2017, *ApJ*, 843, 84
 Palmer, D. M., Barthelmy, S., Gehrels, N., et al. 2005, *Nat*, 434, 1107
 Ravi, V. 2019, *NatAs*, 3, 928
 Scholz, P., Bogdanov, S., Hessels, J. W. T., et al. 2017, *ApJ*, 846, 80
 Scholz, P., Cook, A., Cruces, M., et al. 2020, *ApJ*, 901, 165
 Tavani, M., Casentini, C., Ursi, A., et al. 2021, *NatAs*, 5, 401
 Tavani, M., Verrecchia, F., Casentini, C., et al. 2020, *ApJ*, 893, L42
 Tendulkar, S. P., Bassa, C. G., Cordes, J. M., et al. 2017, *ApJ*, 834, L7
 Tendulkar, S. P., Gil de Paz, A., Kirichenko, A. Y., et al. 2021, *ApJ*, 908, L12
 Tohuvavohu, A., Kennea, J. A., DeLaunay, J., et al. 2020, *ApJ*, 900, 35
 Turolla, R., Zane, S., & Watts, A. L. 2015, *RPPh*, 78, 78116901
 Verrecchia, F., Casentini, C., Tavani, M., et al. 2021, *ApJ*, 915, 102
 Woods, P. M., & Thompson, C. 2006, *Soft Gamma Repeaters and Anomalous X-ray Pulsars: Magnetar Candidates*, Vol. 39 (Cambridge: Cambridge Univ. Press), 547
 Younes, G., Baring, M. G., Kouveliotou, C., et al. 2021, *NatAs*, 5, 408
 Younes, G., Güver, T., Kouveliotou, C., et al. 2020, *ApJ*, 904, L21
 Younes, G., Kouveliotou, C., & Kaspi, V. M. 2015, *ApJ*, 809, 165
 Zhang, B. 2020, *Nat*, 587, 45